Design and implementation of a bacterial signaling circuit

Lazova, M.D.

2013

document version
Publisher's PDF, also known as Version of record

Appendix A

Multiple pathways of opposite chemotactic responses to the cystine / cysteine redox pair in *Salmonella typhimurium*

The chemotaxis system enables motile bacteria to search for an optimum level of environmental factors. Different chemoreceptor species in *Salmonella typhimurium* sense the amino acid cysteine as an attractant and its oxidized dimeric form cystine as a repellent. We investigated the dose-dependent response to cystine and cysteine of *S. typhimurium* using *in vivo* fluorescence resonance energy transfer measurements. Tsr / Tar-mediated response to cysteine has a sigmoidal shape, typical for receptor-ligand interactions. However, the magnitude of the repellent response to cystine scales linearly with the logarithm of cystine concentration over more than four orders of magnitude (20 nM – 500 μM). In contrast to *S. typhimurium* 14028, where we previously observed no response in absence of the McpB / C chemoreceptors, McpB / C-independent responses exist in *S. typhimurium* LT2 even at the very low concentrations in the nanomolar range. We provide a plausible explanation of the linear dependence of the response on the logarithm of cystine concentrations, based on a McpB / C-independent redox-sensing pathway.

Appendix A

A.1. Introduction

Chemotaxis allows bacteria to navigate in gradients of physiologically relevant stimuli, e.g. moving towards higher concentration of nutrients [2,4], lower concentration of toxins [77], or an optimal value of pH [123], oxygen [31], temperature [210] or redox potential [28]. The chemoeffector stimuli are detected by transmembrane receptors, forming allosteric complexes associated with histidine kinase molecules via scaffolding proteins [243,266]. The chemotaxis signaling system has been thoroughly studied in the enteric bacteria *Escherichia coli* and *Salmonella typhimurium*. The receptor-associated kinase CheA's autophosphorylation activity is altered by binding of chemoeffectors to the chemoreceptor clusters. CheA transfers phosphoryl groups to the response regulator CheY, and phosphorylated CheY (CheY-P) interacts with the flagellar motors and alters their rotational bias. The phosphatase CheZ accelerates the dephosphorylation of CheY, and the activity of the receptor-kinase complex is feedback-regulated by a pair of enzymes, CheR and CheB, which add and remove, respectively, methyl groups to specific glutamyl residues of the chemoreceptors.

Chemoreceptors, also called methyl-accepting chemotaxis proteins (MCPs) [1], form homodimers, which in turn assemble into allosteric arrays in the membrane [102]. Chemoreceptor dimers interact at their distal cytoplasmic tips forming trimers of dimers [93,102], which arrange into hexagonal arrays, responsible for the high sensitivity and cooperative nature of chemotaxis signaling [43]. Chemoeffector ligands reversibly bind to the periplasmic domains of the chemoreceptors either directly or via periplasmic binding proteins [185]. Chemoeffector binding induces a conformational change in the periplasmic domain, which is transmitted across the membrane through the regulatory HAMP domain [291], the methyl-accepting domain, and the signal-output domain that regulates the activity of the kinase CheA. Five chemoreceptor species exist in *E. coli*, whereas nine chemoreceptor species exist in *S. typhimurium* (see Table 3.1, Chapter 3). A subset of these MCP species contains a conserved C-terminal pentapeptide motif (NWE^{T}/$_{S}$F) that reversibly binds CheR and CheB, facilitating efficient methylation-dependent adaptation [144]. MCPs have different substrate specificities, with some responding to multiple

chemoeffectors. Conversely, some chemoeffectors are sensed by multiple MCPs (see Table 3.1, Chapter 3). Some chemoreceptor species respond to stimuli via mechanisms other than ligand binding, e.g. Tar and Tsr sense temperature [210]. The relative abundance of each chemoreceptor species depends on the growth conditions and population density [210,284].

The amino acid *L*-cysteine and its oxidized dimeric form *L*-cystine are chemoeffectors of opposing sign for *S. typhimurium* [138] (see Chapter 4). The oxidized and reduced forms are also sensed by different subsets of chemoreceptors: in Chapter 4 [138], we showed that the repellent response to the oxidized form (cystine, abbreviated as CySS) is mediated by McpB and McpC, and the attractant response to the reduced form (cysteine, abbreviated as Cys) is mediated by Tsr and Tar [103,138]. The relative mRNA levels of cystine-sensing receptors McpB and McpC fall between those of the high abundance receptor Tsr and low-abundance receptor Trg, and are similar to those of Tar [267]. McpC does not contain the conserved C-terminal pentapeptide, whereas the C-terminal pentapeptide motif EWVSF in McpB conserves two key residues of the NWE^{T}/$_{S}$F motif [228], and hence is likely to serve as a docking site for the methylation enzymes. The adaptive recovery upon cystine step stimulation has been shown to be incomplete, and the imperfect adaptation has been suggested to promote spreading in motility-plate chemotaxis assays [138].

The opposite responses to cystine and cysteine might provide a mechanism for *S. typhimurium* to find optimal redox conditions and assist the escape of *S. typhimurium* from damage-inducing oxidative environments. Migration to optimal redox conditions, in contrast to movement towards increasing concentration of attractant or decreasing concentration of repellent, cannot be achieved by a monotonic response by a single receptor species, as recently demonstrated for pH taxis and thermotaxis in *E. coli* [210,284]. *E. coli* avoids both highly acidic and highly alkaline conditions by opposing responses of Tar and Tsr: increase of pH elicits an attractant response via Tsr and a repellent response via Tar, and the relative strength of the response is modulated by receptor methylation [122,131,235,259,284]. The sign of the net response is inverted at a well-defined value of pH, which is adjusted in response to changes in cell density. In the motile response to temperature gradients, the opposing responses of Tar

and Tsr lead to accumulation at a preferred point in a temperature gradient: Tsr is responsible for the attraction to warmth and Tar – for the attraction to cold [84,192,210].

Here we investigate the dose-dependent response of *S. typhimurium* to the cystine / cysteine redox pair using *in vivo* fluorescence resonance energy transfer (FRET) measurements. The dose-dependent response to the reduced form, cysteine, is sigmoidal and Tsr / Tar-dependent. However, we show that the oxidized form is sensed by wild type *S. typhimurium* even at very low concentrations (10-20 nM), and the magnitude of the response scales linearly with the logarithm of cystine concentration over more than four orders of magnitude (20 nM – 500 μM). Surprisingly, we detected McpB / C-independent responses to cystine in *S. typhimurium* LT2 strain even at the very low concentrations in the nanomolar range. We observed repellent response in the nanomolar concentration range for another oxidized compound, benzoquinone, and propose an explanation of the linear dependence of the response on the logarithm of cystine concentrations, based on a McpB / C-independent redox-sensing pathway.

A.2. Dose-response relation of the Tar / Tsr -mediated attractant response to cysteine

To characterize the chemotactic signaling response to the reduced form, cysteine, we applied sequential steps of cysteine with increasing concentrations to populations of *S. typhimurium* LT2 cells, immobilized in a flow cell. We measured the output of the chemotaxis system using a fluorescence resonance energy transfer (FRET) assay that utilizes a donor-acceptor pair between the phosphatase CheZ and the response regulator CheY, fused to yellow and cyan fluorescent proteins (YFP and CFP) respectively [226,240-242]. CheY phosphorylation by CheA and its dephosphorylation by CheZ have equal rates at steady state. Thus, the FRET efficiency is proportional to the concentration of the CheZ·CheY-P complex, and this FRET assay provides a measure of the kinase (CheA) activity on time scales longer than the relaxation time of the CheY phosphorylation cycle (~100 ms) [242]. A typical FRET response time series to cystine is shown on Figure A.1A (cysteine is added and removed at times 0

on the left and right panels respectively; note that it takes ~25 s for the cysteine solution to reach the cells after flipping the switch; see Materials and methods). The initial decrease of the FRET level upon addition of cysteine, indicates an attractant response, which is followed by a perfect adaptation to the prestimulus level (see Chapter 4) [138]. Upon removal of cysteine, transient increase in the FRET level followed by a perfect adaptation is observed.

We applied steps of cysteine with increasing concentrations and measured the FRET response in order to characterize the dose-response relation for cysteine in wild type, Δ*tar*, Δ*tsr*, and Δ*tar* Δ*tsr* *S. typhimurium* LT2 strains (Figure A.1B). The dose-response curve for cysteine in wild type *S. typhimurium* shows a sigmoidal shape, with a threshold < 20 μM, half-maximum at ~40 μM and saturation after ~100 μM. Knocking out *tar* does not decrease the amplitude of the response (the slight increase in the amplitudes could be due to experiment-to-experiment variation). However, the amplitude of the saturating response is greatly diminished in the Δ*tsr* strain, confirming that Tsr is the dominant receptor for cysteine at zero cysteine background.

The Δ*tar* Δ*tsr* strain does not show an attractant response to cysteine for any of the tested concentrations. Instead, the FRET level increases upon stimulation by dissolved cysteine (Figure A.1B). A plausible explanation for this repellent-like response to cysteine of the Δ*tar* Δ*tsr* cells is that under the aerobic conditions of our experiments, part of the cysteine oxidizes to cystine (see Section A.2). This effect is not noticeable in wild type cells, where the attractant response to cysteine dominates, but a response in the repellent direction is clearly observed in the cysteine-insensitive Δ*tar* Δ*tsr* cells.

Appendix A

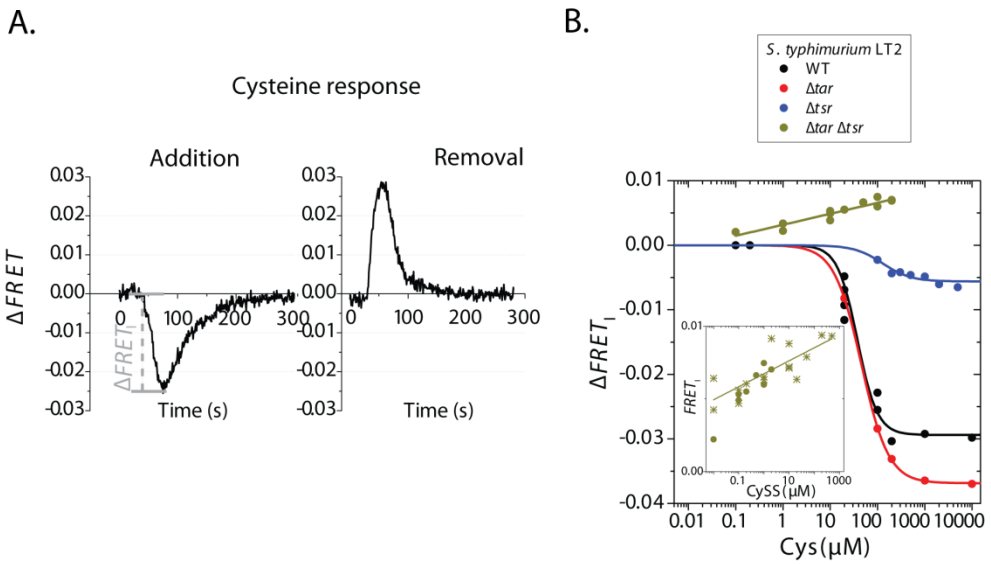

Figure A.1. Attractant response to cysteine of *S. typhimurium* LT2. (A) Typical time series of addition (*left*) and removal (*right*) of cysteine (100 μM) in WT *S. typhimurium*. Cysteine is added and removed at times 0 **(B)** Initial amplitudes of the FRET response ($\Delta FRET_i$) to cysteine of WT, Δ*tar*, Δ*tsr*, and Δ*tar* Δ*tsr* strains are plotted as a function of the cysteine concentration. The respective Hill equation fits with half maximum of 38, 46, and 128 μM, and Hill coefficients of 2.1, 1.5, 1.5 are shown for the first three strains. An apparent linear fit with a slope of 0.017 is shown for the Δ*tar* Δ*tsr* strain. *Inset*: Comparison of the measured response of the Δ*tar* Δ*tsr* strain to cystine (stars) and the expected response to cystine upon stimulation with cysteine solutions in which 1% of the cysteine is oxidized to cystine.

A.3. The magnitude of the repellent response to cystine is proportional to the logarithm of cystine concentration

Cystine, the oxidized molecule in the cystine / cysteine redox pair, elicits a repellent kinase response in *S. typhimurium*: the FRET ratio transiently decreases, followed by a partial (imperfect) adaptation to the prestimulus level (Figure A.2A left) [138]. Upon removal of cystine, the FRET level returns to the prestimulus level in 200-300 s (Figure A.2A right).

We measured the initial amplitudes of the FRET response to a cystine step increase, $\Delta FRET_I$, and plotted them as a function of the added cystine concentration (Figure A.2B). We detected responses to cystine for concentrations as low as 20 nM. For the tested range, 20 nM – 500 μM, the amplitude of the response scales linearly with the logarithm of cystine concentration. We have not explored the response to concentrations of cystine greater than 500 μM because cystine solutions become acidic, and the low pH itself can elicit a chemotaxis response [284].

The shape of the dose-dependent response to cystine is atypical for receptor-ligand binding interactions, which are characterized by linear mass action kinetics or positively cooperative binding, i.e. Hill coefficients $n_H \geq 1$ [80,240,241,248]. Fits with a Hill equation of the cystine dose-response data give Hill coefficients $n_H = 0.50 \pm 0.15$ (these fits were not well constrained, explaining the large fitting error). The atypical shape of the dose-response curve could be a result of multiple receptors with different affinities binding cystine, leading to lower apparent cooperativity of the cystine response [199]. Alternatively, a mechanism that does not involve receptor binding might explain the observed dose-response dependence.

The repellent response to cysteine solutions of the cysteine-insensitive Δ*tar* Δ*tsr* strain scales linearly with the logarithm of cysteine concentration, similar to response to cystine of *S. typhimurium.* The magnitude of the measured responses to cysteine solutions of the cysteine insensitive strain is very similar to the one to cystine solutions with 50-times lower concentration (see Figure A.1, *Inset*). Thus, we conclude that 1% of cysteine in our cysteine solutions might be oxidized to cystine under the aerobic conditions of our experiments (note that two cysteine molecules get oxidized to form one cystine molecule).

Appendix A

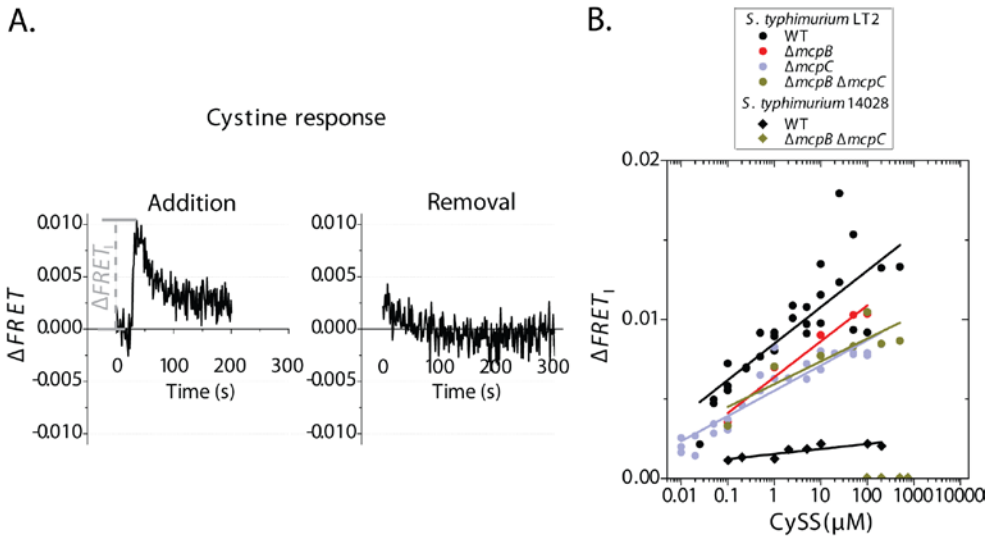

Figure A.2. Repellent response to cystine of *S. typhimurium*. (A) Typical time series of addition (*left*) and removal (r*ight*) of cystine (100 μM) in wild type (WT) *S. typhimurium* LT2. Cystine is added and removed at times 0. **(B)** Initial amplitudes of the FRET response ($\Delta FRET_I$) of WT LT2, Δ*mcpB* LT2, Δ*mcpC* LT2, Δ*mcpB* Δ*mcpC* LT2, WT 14028, and Δ*mcpB* Δ*mcpC* 14028 strains are plotted as a function of the cystine concentration. The apparent linear fits for the first four strains have slopes of 0.0023, 0.0023, 0.0016, 0.0014, and 0.0006 respectively. Δ*mcpB* Δ*mcpC* 14028 does not respond to cystine in the tested concentration range.

A.4. McpB / C knockouts do not affect the shape of cystine dose-response curve in *S. typhimurium* LT2

We showed previously [138] (Chapter 4) that two chemoreceptors of *S. typhimurium*, McpB and McpC, sense cystine as a repellent: deletion of both receptors in *S. typhimurium* 14028 completely abolished the repellent response to cystine (see Figure 4.5, Chapter 4). If there are two receptors that bind ligand independently with different affinities, the net response might be characterized with apparent negative cooperativity, *i.e.* Hill coefficient $n_H < 1$ [199]. The receptors with higher affinity ligand-binding sites will bind the ligand first, but as the concentration of ligand is increased, the receptors with lower affinity binding sites will also bind the ligand, producing an apparent $n_H < 1$. Thus, cystine binding to McpB and McpC with different affinities might explain the shape of the observed dose-response curve. To test this hypothesis, we measured the dependence of $\Delta FRET_I$ on the cystine concentration in Δ*mcpB*, Δ*mcpC*, and Δ*mcpB* Δ*mcpC* *S. typhimurium* LT2 mutant strains. Unexpectedly, the thresholds of cystine response for all tested strains are < 100 nM, and a linear dependence of the amplitude of their response with the logarithm of cystine concentration is observed (Figure A.2B).

The responses of the Δ*mcpB* Δ*mcpC* *S. typhimurium* LT2 strain to cystine contrasts with our previous finding that a Δ*mcpB* Δ*mcpC* *S. typhimurium* 14028 strain does not respond to cystine [138] (Figure A.2B). This finding suggests that a McpB / C-independent mechanism of cystine sensing exists in *S. typhimurium* LT2, which might not exist in *S. typhimurium* 14028. We tested the response to cystine of wild type *S. typhimurium* 14028. Despite the fact that the amplitudes of the cystine response are smaller than those of LT2, we also observe in wild type 14028 a linear scaling of the response with the logarithm of cystine concentration (Figure A.1B). We also observed responses to cystine at concentrations below < 100 nM in both LT2 and 14028 wild type strains.

Unlabeled *cheY* and *cheZ* are present on the genome of the 14028 strains used in our studies, in addition to the *cheY-yfp* and *cheZ-cfp* genes on the plasmid for expression of the FRET pair, and competitive interactions of labeled and unlabeled CheY and CheZ might explain the smaller

amplitudes of the response of the 14028 strains (see Figure 4.6, Chapter 4). Another explanation of the smaller amplitudes of the response of *S. typhimurium* 14028 might be different expression levels of some of the chemotaxis network components between LT2 and 14028 strains [138]. Since the amplitudes of the FRET response of the 14028 strain are in general much smaller than those of the LT2 strain (Figure A.2B) we cannot exclude the possibility that there are small-amplitude responses in the Δ*mcpB* Δ*mcpC* 14028 strain that we are unable to detect at the finite signal-to-noise ratio of these FRET experiments.

A.5. The response to another oxidized redox component, benzoquinone, is similar to the cystine response at low concentrations

The dose-response measurements in *S. typhimurium* LT2 *mcpB* / *C* knockout strains (Figure A.2) suggest the existence of an McpB / C–independent cystine-sensing mechanism in *S. typhimurium*, which magnitude scales linearly with the logarithm of cystine concentration over the whole tested range of concentrations (100 nm – 500 μM for the Δ*mcpB* Δ*mcpC* strain). The latter observation precludes mechanisms in which the response is dependent on ligand-binding to chemoreceptors by linear mass action kinetics or positively cooperative binding [80,240,241,248].

Cystine is a dimeric amino acid, formed by oxidation of the sulfhydryl (-SH) groups of two cysteine monomers, leading to the formation of a disulfide bridge (-S-S-) by a redox reaction

$$cysteine + cysteine + 1/2\, O_2 \rightleftarrows cystine + H_2O$$

It has been shown previously that redox molecules, such as substituted quinones, elicited redox taxis responses: in a spatial redox gradient, bacteria migrate towards a preferred redox potential, and these responses depend mainly on the Aer receptor in *E. coli* [28,202]. Under aerobic conditions, the oxidized forms in the tested quinone redox pairs were sensed as repellents [28]. Our FRET experiments, which were also performed under aerobic conditions, confirmed the latter observation: the oxidized compound benzoquinone elicited a repellent response (note that the reduced form, hydroquinone, also elicited repellent responses, but only for concentrations ≥100 μM; because of its toxicity at high concentrations [258] we

have not explored the hydroquinone response further). Figure A.3A shows a typical time series of a response to benzoquinone. The response to benzoquinone is similar to the repellent response to cystine: both components elicit a repellent response upon a step addition (the FRET level increases), followed by an imperfect adaptation (Figure A.2A and A.3A). Moreover, responses to both compounds were detected at very low concentrations: 1 nM for benzoquinone and 10-20 nM for cystine, and the dose-response dependences for both cystine and benzoquinone appear to scale proportionately with the logarithm of the concentration over the tested range (Figures A.2B and A3.B). We were not able to test benzoquinone concentrations larger than 1 μM because the compound is toxic to the bacteria at high concentrations [258] and its optical activity interferes with the fluorescence levels of the FRET sensors.

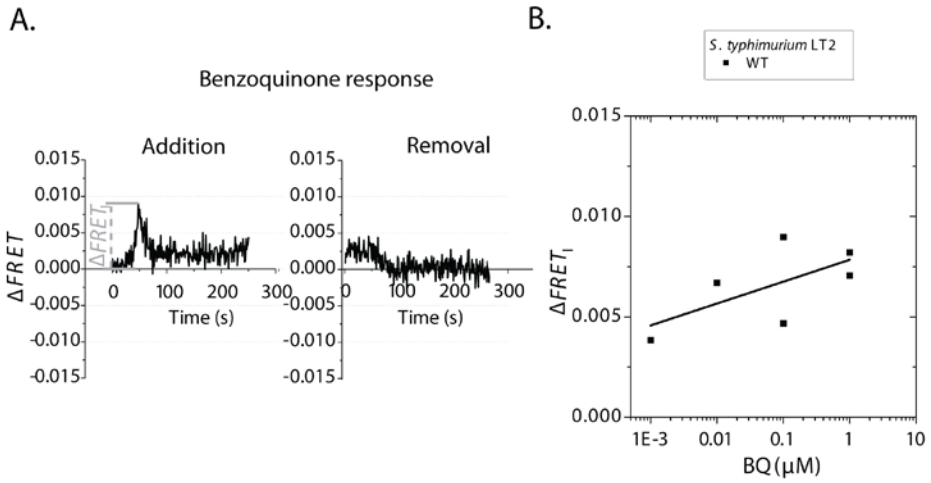

Figure A.3. Repellent response to benzoquinone of *S. typhimurium* LT2. (A) Typical time series of addition (left) and removal (right) of benzoquinone (0.1 μM) in WT *S. typhimurium* LT2. Benzoquinone is added and removed at times 0. **(B)** Initial amplitudes of the FRET response ($\Delta FRET_I$) to benzoquinone of WT *S. typhimurium* are plotted as a function of the benzoquinone concentration. The apparent linear fit has a slope of 0.0011.

Appendix A

A.6. The sign of the response to mixed cystine / cysteine solutions depends on their redox potential

In order to evaluate the redox-dependence of the chemotactic response to cystine / cysteine redox pair, we probed the response of wild type *S. typhimurium* LT2 to defined mixtures of cysteine and cystine at different ratios. (We accounted for 1% interconversion of cysteine to cystine in all cysteine solutions; see Section A.2 and Figure A.1, *Inset*).

We plotted the initial amplitude of the FRET response, $\Delta FRET_I$, for each mixture against $\log Q$, where Q is the reaction quotient of Cys / CySS interconversion reaction, *i.e.* $Q = [CySS]/[Cys]^2$ (Figure A.4; cysteine concentration is squared because two molecules participate in each oxidation reaction). The values of $\log Q$ are proportional to the changes in the redox potentials of the cystine / cysteine solutions, which can be determined by the Nernst equation:

$$E_h = E_0 + 2.3\frac{RT}{nF}\log Q,$$

where E_h is the redox potential of the solution, E_0 is the standard redox potential of the cystine / cysteine redox reaction, R is the gas constant, T is the absolute temperature, n is the number of moles of electrons transferred in the half redox reaction, F is the Faraday constant and Q is the reaction quotient of the redox reaction. For the cystine / cysteine redox pair under the conditions of our experiments (room temperature, neutral pH), the redox potential (V) is

$$E_h = -250 + 30\log Q$$

For values of $\log Q < 100$ the FRET efficiency was found to decrease, indicating an attractant response. For values of $\log Q > 100$ the FRET efficiency was found to increase, indicating a repellent response. Thus, cystine / cysteine mixtures appear to elicit either an attractant or a repellent response depending on the value of $\log Q$, *i.e.* the redox potential of the solutions. Attractant response is observed for more reducing conditions, and repellent response is observed for more oxidizing conditions. Further experiments with defined cystine / cysteine mixtures with $\log Q$ within the range 10 – 1000 could be performed to confirm that the transition between attractant and repellent responses is redox-dependent.

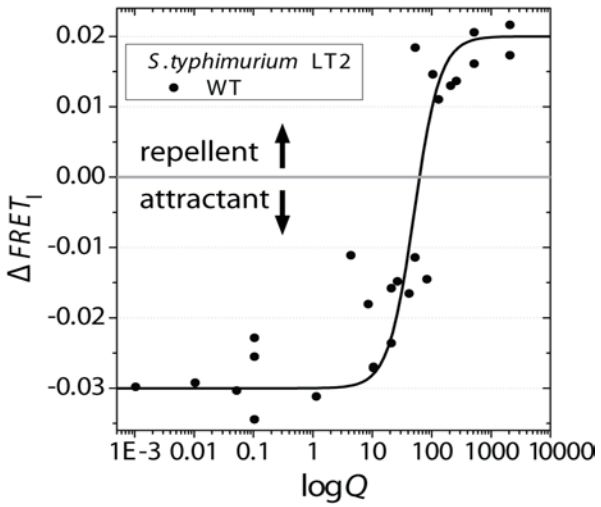

Figure A.4. Response of *S. typhimurium* to cystine / cysteine mixtures. Dependence of the initial amplitude of the FRET response, $\Delta FRET_I$, of wild type (WT) *S. typhimurium* LT2 to the redox potential, expressed in units of $\log Q$, were Q is the reaction quotient of Cys / CySS interconversion. A Hill equation fit (with Hill coefficient of 2 and half-maximum of 51) is shown for guidance of the eye. The grey line at 0 divides attractant (negative) and repellent (positive) responses.

A.7. Discussion

Motile bacteria often implement more than one pathway of sensing in order to orient in a gradient and find an optimal environmental niche. For example, thermotaxis and pH taxis responses both implement different receptors for sensing positive or negative changes from the optimal temperature and pH, respectively [210,284]. We found that the response of *S. typhimurium* to the cystine / cysteine redox pair is mediated by different pathways. Tsr / Tar sense the reduced form (cysteine) as an attractant (Figure A.1). Our earlier measurements of the FRET response of *S. typhimurium* 14028 strain showing that the response is abolished in Δ*mcpB* Δ*mcpC* cells suggested that the cystine response is McpB / C-dependent [138] (Chapter 4). However, our FRET measurements in

S. typhimurium LT2 showed that McpB / C-independent responses exist even at concentrations as low as 100 nM (Figure A.2B).

A plausible explanation for the observed discrepancy of the cystine response of Δ*mcpB* Δ*mcpC* cells is that here and in Chapter 4 [138] we used different *S. typhimurium* strains to evaluate the role of McpB / C in the cystine response: the commonly used lab strain LT2 and the ATCC strain 14028 respectively. LT2 and 14028 shared a common ancestor about 3000 to 9000 years ago, and the 14028 strain is more virulent [89,112]. Their genomes are very similar (>98%) and the alignment of chemotaxis receptor nucleotide sequences show no difference between the two strains. However, it is possible that the McpB / C-independent pathway has different properties in the two strains: since its divergence, the highly virulent 14028 strain accumulated 10% more base substitutions (spread genome-wide, primarily in non-synonymous sites) compared to the virulence-attenuated LT2 strain [112]. The apparent loss of the cystine response in the 14028 strain [138] but not in the LT2 strain upon deletion of both *mcpB* and *mcpC* might also be an artefact resulting from the finite signal-to-noise ratio of our FRET assay: the generally low amplitude of the FRET response of 14028 strains might render responses in the Δ*mcpB* Δ*mcpC* 14028 strain indistinguishable from the noise floor of the FRET measurement.

The shape of the dose-response dependence of *S. typhimurium*'s response to cystine is atypical for receptor-ligand binding: the magnitude of the response scales linearly with the logarithm of the cystine concentration over a very broad concentration range (20 nM – 500 μM). We propose that these responses are part of a redox-sensing pathway, based on our observations of similar responses to another oxidized compound, benzoquinone (Figure A.3). Redox-dependent inversion of the sign of the response to mixtures of cystine and cysteine (Figure A.4) further suggests that a redox-dependent cystine-sensing pathway might exist. However, the results shown on Figure A.4 should be complemented with further measurements of the response to cystine / cysteine mixtures with $\log(Q) = (10 – 1000)$ in order to confirm that the inversion of the response is caused by the redox potential of the mixtures.

The redox responses in *S. typhimurium* could be mediated by Aer as shown for *E. coli* [202], or other redox-sensing receptors might exist: there are

five *S. typhimurium* chemoreceptors that do not exist in *E. coli* (McpB, McpC, Tcp, Tip and the cytosolic receptor McpA, where the function of McpA and Tip is unknown; see Table 3.1, Chapter 3).

What could be the physiological relevance of the multiple pathways of response to the cystine / cysteine redox pair in *S. typhimurium*? Redox potential is an environmental factor that strongly affects cellular metabolism, and it has been hypothesized that redox taxis could guide bacterial species to niches with optimal redox conditions for different metabolic processes, such as hydrogen utilization and nitrogen fixation [28]. Moreover, highly oxidizing conditions lead to a production of free oxygen radicals and oxidative stress, *i.e.* damage to DNA, lipids and proteins [205], and therefore can be detrimental for cells. Creating an oxidative microniche surrounding the macrophage cells is a strategy commonly used by the immune system of the host [111,162], and an active mechanism of avoiding such microenvironments could promote the survival of *S. typhimurium* in the host.

Detection of cysteine as an attractant could also be beneficial for the cells, as cystine is a sulphur-containing nutrient source, and participates in various metabolic pathways. Another advantage of having several pathways for cystine / cysteine sensing is that it could allow bacteria to adjust their "preference" to match the requirements of the cells, by changing the expression levels of some of the chemoreceptors, as observed e.g. for pH taxis and thermotaxis [210,284]. Future studies of the behaviour of *S. typhimurium* in defined cystine / cysteine microenvironments (see Chapter 6) and animal models could shed light on the relevance cystine / cysteine sensing for *S. typhimurium* survival and pathogenesis.

A.8. Materials and methods

Bacterial strains, plasmids and growth conditions

All strains and plasmids used in this work are listed in Table A.1.

CheY-YFP and CheZ-CFP fusions for the FRET experiments were expressed from a plasmid pVS88 [240], induced with 150 μM isopropyl β-D-1-thiogalactopyranoside (IPTG). In the strains used in FRET experiments,

except the strains from R. Harshey's lab (Table A.1), chromosomal *cheY* and *cheZ* were deleted, in order to prevent a competitive interaction between labelled CheY-YFP and CheZ-CFP, and unlabelled CheY and CheZ, expressed from the chromosome, which would lead to a smaller amplitude of the FRET response [138].

Strain	**Relevant genotype**			**Source**
LT2	*Salmonella enterica* serovar Typhimurium strain LT2 (wild type *S. typhimurium* LT2)			*Salmonella* Genetic Stock Center (SGSC)
TSS500	LT2 Δ*cheY* Δ*cheZ*			[138]
TSS878	LT2 Δ*tar* Δ*cheY* Δ*cheZ*			[138]
TSS868	LT2 Δ*tsr* Δ*cheY* Δ*cheZ*			[138]
TSS866	LT2 Δ*tar* Δ*tsr* Δ*cheY* Δ*cheZ*			[138]
TSS941	LT2 Δ*mcpB* Δ*cheY* Δ*cheZ*			This work
TSS942	LT2 Δ*mcpC* Δ*cheY* Δ*cheZ*			This work
TSS958	LT2 Δ*mcpB* Δ*mcpC* Δ*cheY* Δ*cheZ*			This work
14028	wild type *S. typhimurium* ATCC strain 14028			R.M. Harshey
SM542	14028 Δ*mcpB* Δ*mcpC*			[138]
Plasmid	**Gene(s)**	**Resistance**	**Induction**	**Source**
pVS88	*cheZ-ecfp* / *cheY-eyfp*	ampicillin	IPTG	[240]

Table A.1. Strains and plasmids used in this study.

In-frame deletion of genes in the strains designed for this study was achieved by allele-replacement procedure based on Datsenko and Wanner's method [62]. The initial deletion step involved an insertion of a cassette that provides kanamycin resistance, and also contains the lethal gene *ccdB* under the control of *L*-rhamnose inducible promoter, allowing the cassette to be removed by positive selection on *L*-rhamnose-minimal plates [288]. *Salmonella*'s resident plasmid pSLT contains a *ccdA ccdB* operon that interferes with the deletion strategy. Thus, pSLT was displaced prior to allele replacements using Kit10 from *Salmonella* Genetics Stock Collection (SGSC): a plasmid pLL6, which is from the same compatibility group as pSLT, was transformed in the strains of interest, pSLT was cured, and pLL6 was subsequently removed using temperature selection [118].

In all experiments cells were grown at 33.5º C to mid-exponential phase (OD_{600} ~ 0.5) in tryptone broth (TB) (1% Bacto tryptone, 0.5% NaCl, pH 7.0), supplemented with appropriate antibiotics and inducers (Table A.1). Bacteria were harvested by centrifugation, washed and resuspended twice in motility buffer (10 mM potassium phosphate buffer pH 7.0, 0.1 mM EDTA, 1 μM *L*-methionine, 10 mM lactic acid, pH 7.0), and stored at 4° C 1-5 h prior to the experiment.

Chemoeffector preparation

Chemoeffector solutions were prepared as follows. A stock solution of 500 mM cystine (*L*-cystine, Calbiochem, 99.1%, with a certified synthetic origin) was prepared in 1 M HCl because of the poor solubility of cystine in water. Working dilutions were prepared in motility buffer. It has been reported previously that cystine dissolved directly in motility buffer (without using HCl) also elicits a repellent response [138]. Cysteine (*L*-cysteine, Sigma Aldrich, from non-animal source) 100 mM stock and dilutions were prepared directly in motility buffer. The stocks of all other chemoeffectors were made directly in motility buffer. The stock solutions and dilutions of all chemoeffectors were freshly prepared on the day of the FRET experiment (1-3 h prior to the experiment).

Fluorescence resonance energy transfer (FRET) experiments and data analysis

In vivo FRET microscopy on live bacterial populations was performed as described previously [242]. Bacteria, expressing the FRET donor-acceptor pair CheZ-CFP / CheY-YFP, were immobilized on a poly-*L*-lysine–coated microscope coverslip, attached to the top surface of a flow cell [27], and kept under constant flow of motility buffer, generated by a syringe pump (Harvard Apparatus, PHD2000). During the experiment chemoeffectors were added and removed by continuous flow, alternating between solutions using a switch valve (Hamilton). There is a nearly constant delay of ~25 s between the time in which the change of solutions is induced by switching the valve (indicated as time 0 in the figures) and the time, when the new solution reaches the bacteria at the flow cell.

Appendix A

FRET microscopy on bacterial populations was performed on an upright microscope (Nikon FN1), equipped with an oil immersion objective (Nikon CFI Plan Fluor, 40x/1.3). The bacteria in the flow cell were illuminated by a metal halide arc lamp with closed-loop feedback (EXFO X-Cite *exacte*) through an excitation bandpass filter (Semrock, FF01-438/24-25) and a dichroic mirror (Semrock, FF458-Di01). The epifluorescent emission was split by a second dichroic mirror (Semrock, FF509-FDi01) into donor (cyan, C) and acceptor (yellow, Y) channels. The signals from the C and Y channels, passed through emission bandpass filters Semrock FF01-483/32 and FF01-542/27 respectively, were collected by photon-counting photomultipliers (Hamamatsu H7422P-40). Signal intensities were recorded through a data acquisition card (National Instruments) installed on a PC, running custom-written software.

The ratio R between the coverslip background-corrected Y and C fluorescence signal intensities: $R = Y/C$, provided an indicator of FRET activity, robust to fluctuations in the intensity of the light. The change in FRET activity upon stimulation, $\Delta FRET$, can be expressed as a function of the change in the ratio ΔR,

$$\Delta FRET = \frac{R_{pre}+\Delta R-R_0}{R_{pre}+\Delta R+|\Delta Y/\Delta C|} - \frac{R_{pre}-R_0}{R_{pre}+|\Delta Y/\Delta C|},$$

where R_{pre} is the pre-stimulus acceptor to donor ratio, $\Delta R = R - R_{pre}$ is the ratio change, R_0 is the acceptor to donor ratio in absence of FRET, and $|\Delta Y/\Delta C|$ is the constant absolute ratio between the changes in the acceptor and donor signals per FRET pair (for the setup in this study, $|\Delta Y/\Delta C| \approx 0.6$) [242]. Under the measurement conditions $R_{pre} + |\Delta Y/\Delta C| \gg \Delta R$; thus $\Delta FRET \sim \Delta R$. ($\Delta FRET$ is expressed in arbitrary units of ΔR throughout the study).

A.9. Acknowledgements

The FRET experiments were performed by Bob Rosier (MSc student, VU University Amsterdam). Prof. Dr. Rasika Harshey (University of Texas, Austin) provided 14028 strains and helpful discussions.